

# SUPERVISED NONLINEAR SPECTRAL UNMIXING USING A POLYNOMIAL POST NONLINEAR MODEL FOR HYPERSPECTRAL IMAGERY

Yoann Altmann, Abderrahim Halimi, Nicolas Dobigeon and Jean-Yves Tourneret

University of Toulouse, IRIT/INP-ENSEEIH, 31071 Toulouse cedex 7, France

{yoann.altmann,abderrahim.halimi,nicolas.dobigeon,jean-yves.tourneret}@enseeiht.fr

## ABSTRACT

This paper studies a hierarchical Bayesian model for nonlinear hyperspectral image unmixing. The proposed model assumes that the pixel reflectances are polynomial functions of linear mixtures of pure spectral components contaminated by an additive white Gaussian noise. The parameters involved in this model satisfy constraints that are naturally expressed within a Bayesian framework. A Gibbs sampler allows one to sample the unknown abundances and nonlinearity parameters according to the joint posterior of interest. The performance of the resulting unmixing strategy is evaluated thanks to simulations conducted on synthetic and real data.

**Index Terms**— Post nonlinear mixing model, hyperspectral images, hierarchical Bayesian analysis, MCMC methods.

## 1. INTRODUCTION

Spectral unmixing (SU) is one of the major issues when analyzing hyperspectral images. SU consists of identifying the macroscopic materials present in an hyperspectral image and quantifying the proportions of these materials in all pixels of the image. Most SU strategies assume that pixel reflectances are linear combinations of pure component spectra. The resulting linear mixing model (LMM) has been widely used in the literature and has provided promising results. However, as explained in [1], the LMM can be inappropriate for some hyperspectral images, such as those containing sand, trees or vegetation areas [2, 3]. Nonlinear mixing models provide an interesting alternative for overcoming the inherent limitations of the LMM. Nonlinear models proposed in the hyperspectral image literature include the bidirectional reflectance-based model proposed by Hapke [4] and the the bilinear models recently studied in [2, 3, 5]. This paper considers a wide class of nonlinear mixing models referred to as *post nonlinear mixing models* (PNMMs). PNMMs are flexible generalizations of the standard LMMs that have been introduced in [6] for source separation problems (see also [7]). In the hyperspectral imagery context, the endmember spectra can be identified as the *sources* whereas the abundances are the *mixing coefficients* involved in the PNMM. This paper addresses the problem of supervised nonlinear spectral unmixing of hyperspectral images using PNMMs. Supervised unmixing means here that the endmembers (the *sources*) are known, whereas the abundances (the *mixing coefficients*) are unknown and have to be estimated.

Prior knowledge regarding the pure spectral components contained in the observed scene is rarely available in practical applications. As a consequence, the endmember spectra have to be extracted directly from the data using an endmember extraction algorithm (EEA). In the last decades, many EEAs have been developed to identify the pure spectral components contained in a hyperspectral image (the reader is invited to consult [8] for a recent review of

these methods). Most EEAs implicitly rely on the LMM and might be inappropriate for nonlinear models such as PNMMs. However, as noticed in [1], geometric EEAs are still adapted to identify endmembers and can be reasonably employed when the mixing model involves nonlinearities. Therefore, this paper proposes to extract the endmembers contained in the hyperspectral image using *vertex component analysis* (VCA) [9]. Once the endmembers have been extracted from the image, we propose to estimate the abundances, the noise variance and the nonlinearity parameters involved in the PNMM using a Bayesian estimation algorithm. Appropriate prior distributions are assigned to the unknown parameters and hyperparameter associated to the PNMM. The standard Bayesian estimators are difficult to be derived directly from the resulting Bayesian model. Thus they are approximated thanks to samples generated by a Markov chain Monte Carlo (MCMC) method.

The paper is organized as follows. Section 2 presents a PNMM for hyperspectral image analysis. Section 3 summarizes the different components of a hierarchical Bayesian model used for unmixing hyperspectral images using the proposed PNMM. Section 4 derives a Gibbs sampler which allows one to sample from the joint posterior distribution of the unknown PNMM parameters. Some simulation results on synthetic and real data are shown and discussed in Section 5. Conclusions are reported in Section 6.

## 2. POLYNOMIAL POST NONLINEAR MIXING MODEL

This section defines the nonlinear mixing model used for hyperspectral image SU. A PNMM is introduced involving linear and quadratic functions of the abundances. Precisely, the  $L$ -spectrum  $\mathbf{y} = [y_1, \dots, y_L]^T$  of a mixed pixel is defined as a nonlinear transformation  $g$  of a linear mixture of  $R$  spectra  $\mathbf{m}_r$  contaminated by additive noise

$$\mathbf{y} = g \left( \sum_{r=1}^R \alpha_r \mathbf{m}_r \right) + \mathbf{n} = g(\mathbf{M}\boldsymbol{\alpha}) + \mathbf{n} \quad (1)$$

where  $\mathbf{m}_r = [m_{r,1}, \dots, m_{r,L}]^T$  is the spectrum of the  $r$ th material present in the scene,  $\alpha_r$  its corresponding proportion,  $R$  is the number of endmembers contained in the image and  $g$  is an appropriate nonlinear function. In (1),  $L$  is the number of spectral bands and  $\mathbf{n}$  is an additive independent and identically distributed (i.i.d) zero-mean Gaussian noise sequence with variance  $\sigma^2$ , denoted as  $\mathbf{n} \sim \mathcal{N}(\mathbf{0}_L, \sigma^2 \mathbf{I}_L)$ , where  $\mathbf{I}_L$  is the  $L \times L$  identity matrix. Note that the usual matrix and vector notations  $\mathbf{M} = [\mathbf{m}_1, \dots, \mathbf{m}_R]$  and  $\boldsymbol{\alpha} = [\alpha_1, \dots, \alpha_R]^T$  have been used in the right hand side of (1).

The choice of the nonlinearity  $g$  deserves a specific attention. Polynomials, sigmoidal functions and combinations of polynomial

and sigmoidal nonlinearities have shown interesting properties for source separation [7]. This study focuses on second order polynomial nonlinearities  $g$  defined by

$$g: [0, 1]^L \rightarrow \mathbb{R}^L \\ \mathbf{s} \mapsto [g_1(s_1), \dots, g_L(s_L)]^T$$

with  $\mathbf{s} = [s_1, \dots, s_L]^T$  and

$$g_i: [0, 1] \rightarrow \mathbb{R} \\ s_i \mapsto g_i(s_i) = s_i + bs_i^2 \quad (2)$$

for  $i = 1, \dots, L$ . An interesting property of the resulting nonlinear model referred to as polynomial post nonlinear mixing model (PPNMM) is that it reduces to the classical LMM for  $b = 0$ . Thus, we can expect unmixing results at least as good as those presented in [10] for supervised SU. Another motivation for using the PPNMM is the Weierstrass approximation theorem which states that every continuous function defined on an interval can be uniformly approximated by a polynomial with any desired precision [11, p. 15]. As explained in [3], it is reasonable to consider polynomials with first and second order terms (since higher order terms can generally be neglected) which leads to (2). Straightforward computations allow one to express the PPNMM observation vector (for a given pixel of the image) as follows

$$\mathbf{y} = \mathbf{M}\boldsymbol{\alpha} + b(\mathbf{M}\boldsymbol{\alpha}) \odot (\mathbf{M}\boldsymbol{\alpha}) + \mathbf{n} \quad (3)$$

where  $\odot$  denotes the Hadamard product. Note that the resulting PPNMM includes bilinear terms such as those considered in [5].

By studying the derivative of  $g_i$ , it is straightforward to show that the nonlinearity parameter  $b$  must be lower bounded by  $b_{\min} = -0.5$  to make  $g$  invertible. Moreover, due to physical considerations, the abundance vector  $\boldsymbol{\alpha}$  satisfy the following positivity and sum-to-one constraints

$$\sum_{r=1}^R \alpha_r = 1, \quad \alpha_r \geq 0, \forall r \in \{1, \dots, R\}. \quad (4)$$

### 3. HIERARCHICAL BAYESIAN MODEL

This section generalizes the hierarchical Bayesian model introduced in [10] to the PPNMM. The unknown parameter vector associated to the PPNMM contains the pixel abundances  $\boldsymbol{\alpha}$  (satisfying the constraints (4)), the nonlinearity parameter  $b$  and the additive noise variance  $\sigma^2$ . This section summarizes the likelihood and the parameters priors associated to the proposed hierarchical Bayesian PPNMM.

#### 3.1. Likelihood

Equation (3) shows that  $\mathbf{y}|\boldsymbol{\alpha}, b, \sigma^2 \sim \mathcal{N}(g(\mathbf{M}\boldsymbol{\alpha}), \sigma^2 \mathbf{I}_L)$ . As a consequence, the likelihood function of  $\mathbf{y}$  can be expressed as

$$f(\mathbf{y}|\boldsymbol{\alpha}, b, \sigma^2) = \left( \frac{1}{2\pi\sigma^2} \right)^{\frac{L}{2}} \exp\left( -\frac{\|\mathbf{y} - g(\mathbf{M}\boldsymbol{\alpha})\|^2}{2\sigma^2} \right) \quad (5)$$

where  $\|\mathbf{x}\| = \sqrt{\mathbf{x}^T \mathbf{x}}$  is the standard  $\ell^2$  norm for a vector  $\mathbf{x} \in \mathbb{R}^L$ .

#### 3.2. Parameter and hyperparameter priors

In order to satisfy the sum-to-one constraint, the abundance vector can be rewritten  $\boldsymbol{\alpha} = [\boldsymbol{\alpha}_{-k}, \alpha_k]^T$  with  $k \in \{1, \dots, R\}$ ,  $\boldsymbol{\alpha}_{-k} = [\alpha_1, \dots, \alpha_{k-1}, \alpha_{k+1}, \dots, \alpha_R]^T$  and  $\alpha_k = 1 - \sum_{r=1, r \neq k}^R \alpha_r$ . The positivity constraints in (4) impose that  $\boldsymbol{\alpha}_{-k}$  belongs to the following simplex  $\mathcal{S}_k$

$$\mathcal{S}_k = \left\{ \boldsymbol{\alpha}_{-k} \mid \alpha_r \geq 0, \forall r \neq k, \sum_{r \neq k} \alpha_r \leq 1 \right\}. \quad (6)$$

A uniform prior distribution on  $\mathcal{S}_k$  is chosen for  $\boldsymbol{\alpha}_{-k}$  to reflect the absence of prior knowledge about the abundance vector.

A conjugate inverse-gamma prior is chosen for  $\sigma^2$

$$\sigma^2 \mid \nu, \gamma \sim \text{IG}\left(\frac{\nu}{2}, \frac{\gamma}{2}\right) \quad (7)$$

where the hyperparameter  $\nu$  is fixed to  $\nu = 2$  whereas  $\gamma$  is included within the Bayesian model. This prior has shown interesting properties in many practical applications [10, 12].

As explained above, the nonlinearity parameter  $b$  is lower bounded by  $b_{\min} = -0.5$  to make the nonlinear transformation  $g$  invertible. The parameter  $b$  is also assumed to be upper bounded by a real parameter  $\delta$  characterizing the importance of the nonlinearity  $g$  (indeed, the larger  $\delta$ , the larger the distance between  $g$  and the identity function). A uniform prior distribution on  $\mathcal{D}_\delta = [-0.5, \delta]$  is finally assigned to the nonlinear parameter  $b$ .

A Jeffreys' prior is assigned to the hyperparameter  $\gamma$

$$f(\gamma) \propto \frac{1}{\gamma} \mathbf{I}_{\mathbb{R}^+}(\gamma) \quad (8)$$

where  $\mathbf{I}_{\mathbb{R}^+}(\cdot)$  is the indicator function defined on  $\mathbb{R}^+$  (see [10, 12] for motivations).

#### 3.3. Posterior distribution of $\boldsymbol{\theta}$

The following hierarchical structure allows one to compute the posterior distribution of the unknown parameter vector  $\boldsymbol{\theta} = \{\boldsymbol{\alpha}_{-k}, b, \sigma^2\}$

$$f(\boldsymbol{\theta}|\mathbf{y}) \propto \int f(\mathbf{y}|\boldsymbol{\theta})f(\boldsymbol{\theta}|\gamma)f(\gamma)d\gamma \quad (9)$$

where  $f(\mathbf{y}|\boldsymbol{\theta})$  and  $f(\gamma)$  are defined in (5) and (8). By assuming the parameters  $\sigma^2$ ,  $b$  and  $\boldsymbol{\alpha}_{-k}$  are *a priori* independent, the posterior distribution  $f(\boldsymbol{\theta}|\mathbf{y})$  can be computed up to a multiplicative constant

$$f(\boldsymbol{\alpha}_{-k}, b, \sigma^2|\mathbf{y}) \propto \frac{1}{\sigma^2} f(\mathbf{y}|\boldsymbol{\alpha}_{-k}, \sigma^2, b) \mathbf{1}_{\mathcal{S}_k \times \mathcal{D}_\delta}(\boldsymbol{\alpha}_{-k}, b) \quad (10)$$

where  $\propto$  means ‘‘proportional to’’. The next section derives an efficient Metropolis-within-Gibbs algorithm allowing one to sample according to the posterior distribution  $f(\boldsymbol{\alpha}_{-k}, b, \sigma^2|\mathbf{y})$ .

### 4. GIBBS SAMPLER FOR NONLINEARITY AND ABUNDANCE ESTIMATION

The principle of the Gibbs sampler is to sample according to the conditional distributions of the posterior of interest [13, p. 371-424]. The conditional distributions associated to the posterior (10) are summarized below.

#### 4.1. Generating samples according to $f(\alpha_{-k}|\mathbf{y}, b, \sigma^2)$

According to the last section, once  $k \in \{1, \dots, R\}$  has been selected, the conditional distribution of  $\alpha_{-k}$  is

$$f(\alpha_{-k}|\mathbf{y}, \sigma^2, b) \propto \exp\left(-\frac{\|\mathbf{y} - g(\mathbf{M}\alpha)\|^2}{2\sigma^2}\right) \mathbf{1}_{S_k}(\alpha_{-k}). \quad (11)$$

To obtain good mixing properties, the abundance vector  $\alpha_{-k}$  is updated coordinate by coordinate thanks to a Metropolis-Hasting move. In this study, a new abundance coefficient is proposed following a Gaussian random walk procedure. The variance of the proposal distribution has been adjusted to obtain an acceptance rate close to 0.5, as recommended in [14, p. 8].

#### 4.2. Generating samples according to $f(b|\mathbf{y}, \alpha_{-k}, \sigma^2)$

Using (5), it can be easily shown that  $b$  is distributed according to the following truncated Gaussian distribution

$$b|\mathbf{y}, \alpha_{-k}, \sigma^2 \sim \mathcal{N}_{\mathcal{D}_b}(\mu, \sigma_b^2) \quad (12)$$

where

$$\mu = \frac{\mathbf{y}^T h(\mathbf{M}, \alpha)}{\|h(\mathbf{M}, \alpha)\|^2}, \quad \sigma_b^2 = \frac{1}{\|h(\mathbf{M}, \alpha)\|^2}$$

and  $h(\mathbf{M}, \alpha) = (\mathbf{M}\alpha) \odot (\mathbf{M}\alpha)$ . Generating samples according to a truncated Gaussian distribution can be achieved as in [15].

#### 4.3. Generating samples according to $f(\sigma^2|\mathbf{y}, \alpha_{-k}, b)$

By considering the posterior distribution (10), it can be shown that  $\sigma^2|\mathbf{y}, \alpha_{-k}, b$  is distributed according to the following inverse-gamma distribution

$$\sigma^2|\mathbf{y}, \alpha_{-k}, b \sim \mathcal{IG}\left(\frac{L}{2}, \frac{\|\mathbf{y} - g(\mathbf{M}\alpha)\|^2}{2}\right). \quad (13)$$

After generating samples using the procedures detailed in Sections 4.1, 4.2 and 4.3, the minimum mean square error (MMSE) estimator of the unknown parameters can be approximated by computing the empirical averages of these samples, after a short burn-in period. The length of the burn-in period has been determined using appropriate convergence diagnoses [14].

## 5. SIMULATION RESULTS

### 5.1. Synthetic data

The performance of the Bayesian estimation procedure is first investigated on a simple example. A synthetic pixel has been generated according to the PPNMM (4) with  $R = 3$  endmembers extracted from the spectral libraries provided with the ENVI software (i.e., construction concrete, green grass and dark yellowish brown micaceous loam), abundances  $\alpha = [0.3, 0.6, 0.1]$  and a nonlinearity coefficient  $b = 0.3$ . The mixture has been corrupted by an additive white Gaussian noise with  $\sigma^2 = 0.0033$ . Using the standard signal to noise ratio definition  $\text{SNR} = L^{-1}\sigma^{-2}\left\|g\left(\sum_{r=1}^R \mathbf{m}_r \alpha_r\right)\right\|^2$ , this value of  $\sigma^2$  yields  $\text{SNR} \approx 15$  dB. As explained before, the prior for the nonlinearity parameter  $b$  is uniform on the interval  $[-0.5, \delta]$ , where  $\delta$  is the only hyperparameter that needs to be adjusted for the proposed model. All simulations presented in this paper have been obtained with  $\delta = 2$  which was determined by cross validation. Fig. 1 shows the estimated posterior distributions of the abundances and

the nonlinearity parameter  $b$  for a Markov chain with  $N_{MC} = 20000$  samples (including  $N_{bi} = 1000$  burn-in iterations). The histograms of the generated samples are clearly in good agreement with the actual values of the model parameters. Fig. 2 shows the abundances and nonlinearity MMSE estimates and the corresponding standard deviations versus SNR (the horizontal red lines indicate the actual values of the parameters). Note that SNRs are not below 30 dB for the actual spectrometers. Consequently, the proposed algorithm provides accurate estimation of all parameters for the SNRs of interest.

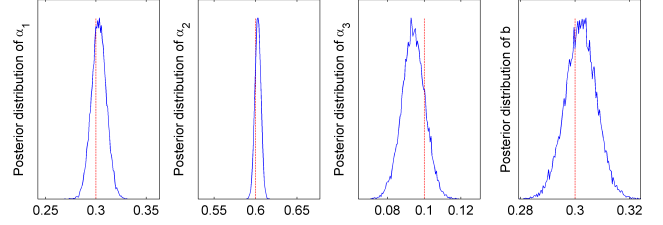


**Fig. 1.** Actual values (vertical red dashed lines) and estimated posterior distributions (blue lines) of the abundances (3 left plots) and the nonlinearity coefficient (right plot).

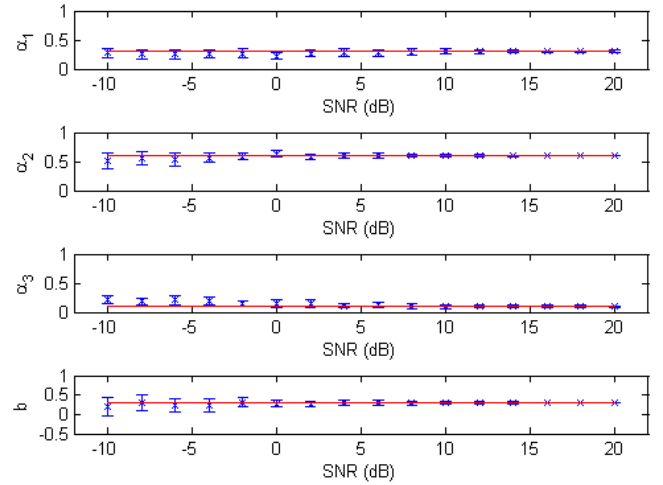


**Fig. 2.** MMSE estimates (cross) and standard deviations (vertical bars) for  $\alpha = [0.3, 0.6, 0.1]^T$  and  $b = 0.3$  versus SNR.

### 5.2. Spectral unmixing of an AVIRIS image

The real image considered in this section is composed of  $L = 189$  spectral bands and was acquired in 1997 by the airborne visible infrared imaging spectrometer (AVIRIS) over the Cuprite mining site in Nevada. A sub-image of size  $50 \times 50$  pixels has been chosen here to evaluate the proposed unmixing procedure. The scene is mainly composed of muscovite, alunite and kaolinite, as explained in [16]. The endmembers are extracted by VCA [9], with  $R = 3$ , and are shown in Fig. 3 (top). The hierarchical Bayesian algorithm presented in Section 4 has been applied independently on each pixel of the scene using the endmembers extracted by VCA. The image abundance maps estimated by the proposed algorithm are presented in Fig. 3 (bottom). They are similar to the abundance maps obtained with a Bayesian algorithm associated to the LMM studied in [10] (middle). However, the advantage of the PPNMM is that it allows one to analyze the nonlinearities between the observations and the

endmembers. For instance, Fig. 4 shows the estimated posterior distribution of  $b$  on the Cuprite image (2500 pixels). These results show that the observations are nonlinearly related to the endmembers (since  $b \neq 0$ ) but that these nonlinearity are weak (the estimated values of  $b$  are close to 0).

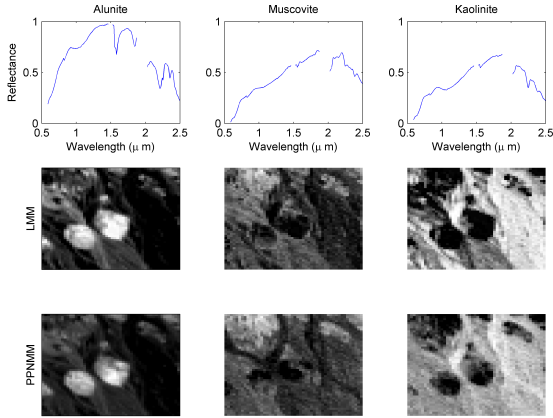


**Fig. 3.** Top: the 3 endmember spectra estimated by the VCA algorithm for the Cuprite scene. Middle: abundance maps for LMM + Bayesian algorithm [10]. Bottom: abundance maps for the proposed PPNMM and Bayesian algorithm.

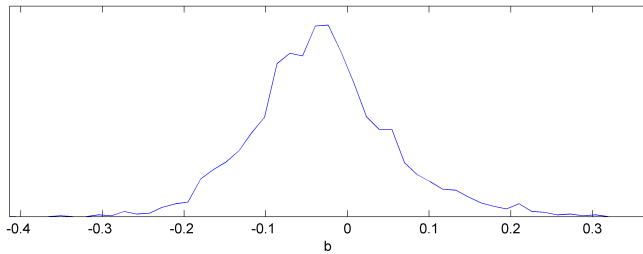


**Fig. 4.** Histogram of the MMSE estimates of  $b$  for the Cuprite image.

**Table 1.** Average MSE for the Cuprite scene.

Fan Model	LMM		PPNLMM
	Bayesian Algo.	FCLS	
$9.31 \times 10^{-4}$	$4.59 \times 10^{-4}$	$4.43 \times 10^{-4}$	$1.42 \times 10^{-4}$

In order to analyze the performance of the proposed PPNMM, the average MSEs between the observed pixels and the model approximations (defined by  $MSE = L^{-1} \|y - g(M\alpha)\|^2$  for the PPNMM and  $MSE = L^{-1} \|y - M\alpha\|^2$  for the LMM) are reported in Table 1 for four different scenarios (bilinear model proposed in [5] + Bayesian algorithm, LMM + Bayesian algorithm [10], LMM + FCLS algorithm [17] and PPNMM + proposed Bayesian algorithm). These results are clearly in favor of the proposed nonlinear model and Bayesian estimation algorithm.

## 6. CONCLUSIONS

A new Bayesian nonlinear unmixing algorithm was presented for hyperspectral imagery. This algorithm assumed that the hyperspectral image pixels are related to the endmembers by a polynomial post-nonlinear mixing model. The constraints related to the unknown parameters of this model were considered by defining appropriate prior distributions. To alleviate the computational complexity of the resulting Bayesian estimators, we derived a Gibbs sampler generating samples asymptotically distributed according to the posterior distribution of the proposed model. The generated samples were then used to estimate the model parameters and measures of uncertainty (confidence intervals) for these estimates. The proposed unmixing strategy provided promising results. Future works include the derivation of nonlinearity detectors based on the proposed model or the study of other nonlinear mixing models for hyperspectral imagery.

## 7. REFERENCES

- [1] N. Keshava and J. F. Mustard, "Spectral unmixing," *IEEE Signal Processing Magazine*, pp. 44–57, Jan. 2002.
- [2] B. Somers, K. Cools, S. Delalieux, J. Stuckens, D. V. der Zande, W. W. Verstraeten, and P. Coppin, "Nonlinear hyperspectral mixture analysis for tree cover estimates in orchards," *Remote Sensing of Environment*, no. 113, pp. 1183–1193, 2009.
- [3] J. M. P. Nascimento and J. M. Bioucas-Dias, "Nonlinear mixture model for hyperspectral unmixing," *Proceedings of the SPIE*, vol. 7477, pp. 74 770I–74 770I–8, 2009.
- [4] B. W. Hapke, "Bidirectional reflectance spectroscopy. I. Theory," *J. Geophys. Res.*, vol. 86, pp. 3039–3054, 1981.
- [5] W. Fan, B. Hu, J. Miller, and M. Li, "Comparative study between a new nonlinear model and common linear model for analysing laboratory simulated-forest hyperspectral data," *Remote Sensing of Environment*, vol. 30, no. 11, pp. 2951–2962, 2009.
- [6] C. Jutten and J. Karhunen, "Advances in nonlinear blind source separation," in *4th Int. Symp. on Independent Component Analysis and Blind Signal Separation (ICA2003)*, 2003, pp. 245–256.
- [7] M. Babaie-zadeh, C. Jutten, and K. Nayebi, "Blind separating convolutive post non-linear mixtures," in *Econometrica*, 2001, pp. 138–143.
- [8] M. Parente and A. Plaza, "Survey of geometric and statistical unmixing algorithms for hyperspectral images," in *Proc. IEEE GRSS Workshop on Hyperspectral Image and Signal Processing: Evolution in Remote Sensing (WHISPERS)*, Reykjavik, Iceland, 2010.
- [9] J. M. Nascimento and J. M. Bioucas-Dias, "Vertex component analysis: A fast algorithm to unmix hyperspectral data," *IEEE Trans. Geosci. and Remote Sensing*, vol. 43, no. 4, pp. 898–910, April 2005.
- [10] N. Dobigeon, J.-Y. Tourneret, and C.-I. Chang, "Semi-supervised linear spectral unmixing using a hierarchical Bayesian model for hyperspectral imagery," *IEEE Trans. Signal Process.*, vol. 56, no. 7, pp. 2684–2695, July 2008.
- [11] V. J. Mathews and G. L. Sicuranza, *Polynomial Signal Processing*. New York: Wiley, 2000.
- [12] E. Puskaya, C. Andrieu, A. Doucet, and W. Fitzgerald, "Bayesian curve fitting using MCMC with applications to signal segmentation," *IEEE Trans. Signal Process.*, vol. 50, no. 3, pp. 747–758, March 2002.
- [13] C. P. Robert and G. Casella, *Monte Carlo Statistical Methods*, 2nd ed. New York: Springer-Verlag, 2004.
- [14] C. P. Robert and D. Cellier, "Convergence control of MCMC algorithms," in *Discretization and MCMC Convergence Assessment*, C. P. Robert, Ed. New York: Springer Verlag, 1998, pp. 27–46.
- [15] C. P. Robert, "Simulation of truncated normal variables," *Statistics and Computing*, vol. 5, pp. 121–125, 1995.
- [16] N. Dobigeon, S. Moussaoui, M. Coulon, J.-Y. Tourneret, and A. O. Hero, "Joint Bayesian endmember extraction and linear unmixing for hyperspectral imagery," *IEEE Trans. Signal Process.*, vol. 57, no. 11, pp. 2657–2669, nov 2009.
- [17] D. C. Heinz and C.-I. Chang, "Fully constrained least-squares linear spectral mixture analysis method for material quantification in hyperspectral imagery," *IEEE Trans. Geosci. and Remote Sensing*, vol. 29, no. 3, pp. 529–545, March 2001.